

XX (2020), 0, 0, pp. 1–21  
doi:XX/XX/TerracesDupBioRxiv

# Terraces in Gene Tree Reconciliation-Based Species Tree Inference

MICHAEL J. SANDERSON<sup>1,\*</sup>, MICHELLE M. MCMAHON<sup>2</sup>, AND MIKE STEEL<sup>3</sup>

<sup>1</sup> Department of Ecology and Evolutionary Biology, University of Arizona, Tucson, AZ 85721, USA

<sup>2</sup> School of Plant Sciences, University of Arizona, Tucson, AZ 85721

<sup>3</sup> Biomathematics Research Centre, University of Canterbury, Christchurch, NZ

*\*Michael J. Sanderson, Dept. of Ecology and Evolutionary Biology, University of Arizona; Tucson, AZ 85721, USA; 520-626-6848; sanderm@email.arizona.edu*

## ABSTRACT

1 Terraces in phylogenetic tree space are sets of trees with identical optimality scores for a  
2 given data set, arising from missing data. These were first described for multilocus  
3 phylogenetic data sets in the context of maximum parsimony inference and maximum  
4 likelihood inference under certain model assumptions. Here we show how the mathematical  
5 properties that lead to terraces extend to gene tree - species tree problems in which the  
6 gene trees are incomplete. Inference of species trees from either sets of gene family trees  
7 subject to duplication and loss, or allele trees subject to incomplete lineage sorting, can  
8 exhibit terraces in their solution space. First, we show conditions that lead to a new kind  
9 of terrace, which stems from subtree operations that appear in reconciliation problems for  
10 incomplete trees. Then we characterize when terraces of both types can occur when the  
11 optimality criterion for tree search is based on duplication, loss or deep coalescence scores.  
12 Finally, we examine the impact of assumptions about the causes of losses: whether they are  
13 due to imperfect sampling or true evolutionary deletion.

14 *Key words:* gene tree reconciliation, terraces, phylogenomics, span

16 A long standing and still largely dominant paradigm in phylogenetic tree inference  
17 is based on optimization of some score derived from data over candidate tree solutions. In  
18 addition to familiar maximum parsimony, maximum likelihood, and (certain)  
19 distance-based methods like minimum evolution and Fitch-Margoliash (Felsenstein 2004),  
20 all commonly used to infer a tree from a sequence alignment, optimization methods also  
21 are employed in a diverse set of methods aimed at solving other tree inference problems,  
22 such as supertree construction, gene tree reconciliation, species tree inference using  
23 likelihood or pseudo-likelihood, and network reconstruction. Computational obstacles in  
24 optimization include the problem of multiple optima and regions where the solution space  
25 is flat, which can both impede algorithms to find optima and make circumscription of  
26 solutions more complex. One contributor to this problem in phylogenetics is missing data,  
27 and a particularly direct example of this is the phenomenon of “terraces”—regions of tree  
28 space having identical optimality scores purely due to certain patterns of missing data  
29 among the taxa sampled (Sanderson et al. 2011, 2015).

30 The properties of terraces have been elucidated mostly in the context of large  
31 multilocus data sets, where the pattern of missing data can be described by the “taxon  
32 coverage” of data—which loci are sampled for which taxa. If a tree is inferred for a  
33 concatenated multilocus alignment by maximum parsimony, or by maximum likelihood  
34 with certain model assumptions, the pattern of taxon coverage alone can be used to infer  
35 the number and sizes of terraces having identical optimality scores. Surveys of empirical  
36 studies indicate that terraces can be astronomically large in large trees (Dobrin et al.  
37 2018), and they can degrade other aspects of phylogenetic inference aside from tree search,  
38 such as estimation of confidence intervals (Sanderson et al. 2015). They are likely to have  
39 an impact on comparative methods and other studies that employ statistical inference  
40 methods that depend on accurate evaluation of the confidence set of trees.

41 The conditions required for terraces to be observed in phylogenetic inference  
42 problems are quite general (Steel 2016). In this paper we describe their impact on a large

43 additional set of phylogenetic problems involving building species trees from gene trees  
44 using gene tree reconciliation methods. This includes methods that have been used to infer  
45 species trees from gene families that have undergone a history of gene duplication and  
46 deletion, as well as methods that have been used to infer species tree from allele trees in  
47 which population genetic processes lead to deep coalescence events. This area is  
48 undergoing active development in the phylogenomics community and our results pertain  
49 most directly to discrete parsimony-like methods arising from the reconciliation  
50 framework, but potential connections to model based approaches may exist by analogy to  
51 previous findings with maximum likelihood in concatenation methods (Sanderson et al.  
52 2011). We find that terraces are not only expected in this new context, but that an  
53 additional *type* of terraces can be seen in certain versions of reconciliation problems.

54 *Trees, Subtrees, and Display*

55 We assume all trees,  $T$ , are rooted, binary, and have edges,  $E(T)$  and nodes,  $V(T)$ ,  
56 and root node,  $r(T) \in V(T)$ . Nodes are partitioned into the set of internal nodes,  $\dot{V}(T)$   
57 (having outdegree two or more), and the set of leaves,  $L(T)$  (having indegree one), each of  
58 which is labeled by a distinct element of the leaf set,  $X$ . If node  $v'$  is an ancestor of  $v$ , we  
59 write  $v' > v$ . The set of leaf labels descended from  $v$  is  $C_T(v)$ . The node of the most recent  
60 common ancestor of a set of leaves,  $A$ , is  $\text{MRCA}_T(A)$ .

61 Given a rooted binary tree,  $T$  with leaf label set,  $X$ , and with  $X_g \subseteq X$ , we define  
62 two kinds of subtrees of  $T$  having leaf label set,  $X_g$  (Fig. 1):

63 1. The “homomorphic subtree”,  $T|_{X_g}$ , is the smallest subtree of  $T$  having leaf label  
64 set  $X_g$  and suppressing any interior nodes with outdegree one (“unary” nodes). When the  
65 context is clear, we abbreviate this to  $T|_g$ .

66 2. The “restriction subtree”,  $T||_{X_g}$ , is the smallest subtree having leaf label set  $X_g$   
67 but keeping any unary nodes. When the context is clear, we abbreviate this to  $T||_g$ .

68 A tree  $T$  *displays* a binary subtree  $g$  having leaf label set  $X_g \subseteq X$  if  $T|_{X_g} = g$  (Steel

69 2016). [If  $g$  is not binary then this definition can be extended to allow  $T|_g$  to be a  
70 refinement (resolution) of  $g$ .] This is the conventional definition of “display”, but it can be  
71 generalized to use the restriction subtree when appropriate (see below).

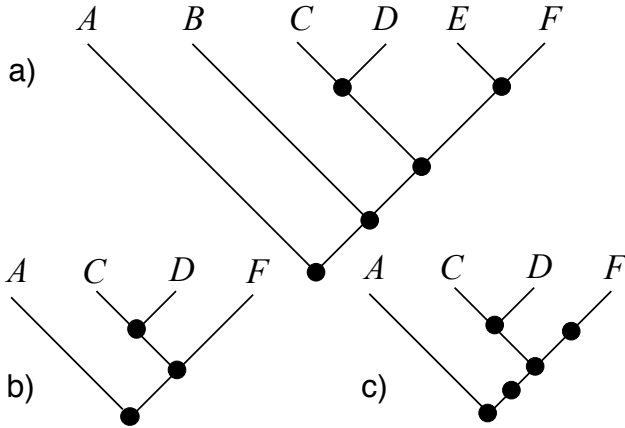


Fig. 1. Illustration of two subtree operations, retaining leaf label set  $X_g = \{A, C, D, F\}$ : a) Original species tree,  $T$ ; b) homomorphic subtree,  $T|_{X_g}$ ; c) restriction subtree,  $T||_{X_g}$ .

72

### Spans and Terraces

73 In general, given a sequence of rooted binary trees,  $\mathcal{T} = (T_1, \dots, T_k)$ , with leaf label  
74 sets  $X_i$  ( $X = \cup_i X_i$ ), define the *span*,  $\langle \mathcal{T} \rangle$ , as the set of all rooted binary trees having label  
75 set  $X$  that display every tree in  $\mathcal{T}$  (Fig. 2). The span may be empty.

76 Consider the special case of a rooted binary *parent tree*,  $T$ , with leaf label set,  $X$ ,  
77 along with a sequence of leaf label subsets,  $\chi = (X_1, \dots, X_k)$ ,  $X_i \subseteq X$ . Label set  $X_i$  may be  
78 thought of as the set of leaves present in a subtree of  $T$  or as the set of leaves of  $T$  that  
79 have some kind of data present, say the sequence of the  $i$ th gene in a multigene multiple  
80 sequence alignment. Let  $\mathcal{T}|_\chi = (T|_{X_1}, \dots, T|_{X_k})$ , then  $\langle \mathcal{T}|_\chi \rangle$  is the span of this sequence of  
81 subtrees derived from the parent tree (Fig. 2). Clearly the size of this span is at least one  
82 since it contains  $T$ .

83 A *terrace* is a span,  $\langle \mathcal{T}|_\chi \rangle$ , in which all the trees have the same *score*. The  
84 properties of this score determine whether this is a possibility. Given some cost function,

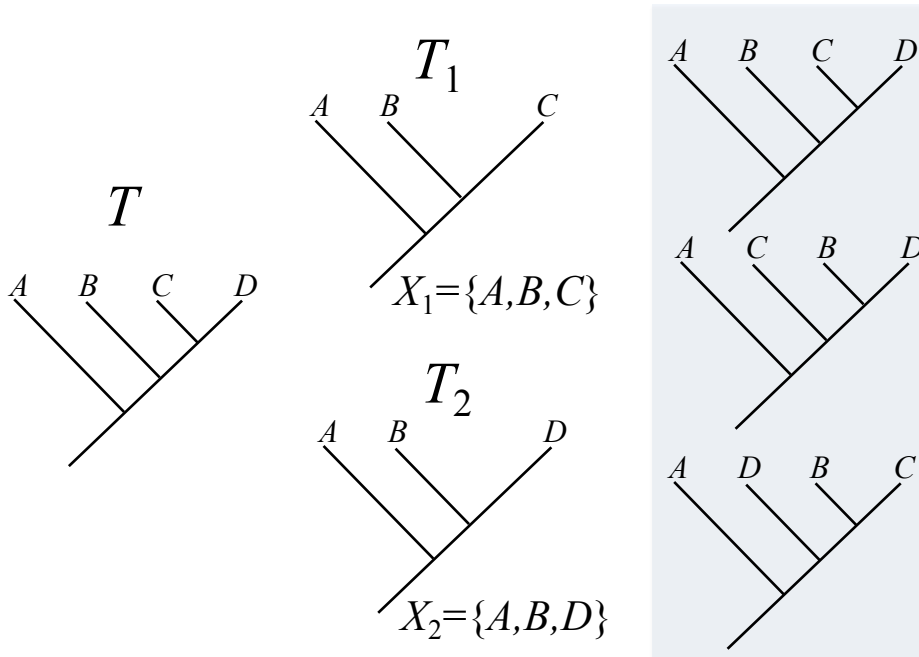


Fig. 2. Span of a set of subtrees. Original rooted parent tree is  $T$  having leaf label set,  $X = \{A, B, C, D\}$ . Subsets of label sets,  $X_1$  and  $X_2$ , induce a sequence of subtrees,  $\mathcal{T}|_X = (T|_{X_1}, T|_{X_2}) = (T_1, T_2)$ . Each of the trees on  $X$  in the shaded box displays both  $T_1$  and  $T_2$  and this set of three trees is the *span* of  $\mathcal{T}|_X$ ,  $\langle \mathcal{T}|_X \rangle$ .

85  $c(S, g)$  for a tree,  $T$ , with leaf label set,  $X$ , based on some data associated with “gene”,  $g$ ,  
86 valid even if only a subset of leaves,  $X_g \subseteq X$ , have data present; and given some score  
87 function,  $s(c(T, g_1), \dots, c(T, g_m))$ , that combines these costs across a set of genes,  
88  $\mathcal{G} = \{g_1, \dots, g_m\}$ , the following two properties of  $c$  and  $s$  are sufficient to cause all trees in  
89 the span to have the same score (Sanderson et al. 2011; Steel 2016):

90 *Condition 1.* The cost function is the same on the full tree as it is on the subtree  
91 pruned to those taxa that have data.

$$c(T, g) = c(T|_{X_g}, g). \quad (1)$$

92 *Condition 2.* The score function,  $s$ , is a linear sum of costs for each gene:

$$s(T, \mathcal{G}) = \sum_i c(T, g_i). \quad (2)$$

93 **Theorem 1** (Terraces—Type I). *If the score function,  $s$ , satisfies the two conditions  
94 described above, then every tree in the span,  $\langle \mathcal{T}|_X \rangle$ , has the score,  $s(T, \mathcal{G})$ .*

95 *Proof.* Following Steel (2016), if  $T' \in \langle \mathcal{T} | \chi \rangle$ , Then  $T'|_{X_i} = T|_{X_i}$  for  $i = 1, \dots, k$ , so

$$s(T', \mathcal{G}) = \sum_i c(T', g_i) = \sum_i c(T'|_{X_i}, g_i) = \sum_i c(T|_{X_i}, g_i) = \sum_i c(T, g_i) = s(T, \mathcal{G}) \quad (3)$$

96  $\square$

97 This is most interesting if  $|\langle \mathcal{T} \rangle| >> 1$ . In fact, the size of terraces can be  
98 astronomically large for some data sets for large parent trees (Sanderson et al. 2011;  
99 Dobrin et al. 2018) when there is a sizable amount of missing data.

100 In Sanderson et al. (2011, 2015) and Steel (2016) the data set associated with gene  
101  $g$  was taken to be a multiple sequence alignment over some block of sites, and the scores  
102 considered included maximum parsimony and maximum likelihood scores. The exact  
103 circumscription of “blocks” is relevant, but for simplicity we conceptualize it as data  
104 associated with a single gene in the genome (see Sanderson et al. 2015).

105 *Terraces—Type II*

106 We now show that terraces arise when using the restriction subtree operation,  
107 which will be relevant for discussion of gene tree reconciliation below.

108 Define a “restriction span” by (i) using the restriction subtree in the above  
109 definition of “display”, and then (ii) letting  $\mathcal{T}||_{\chi} = (T||_{X_1}, \dots, T||_{X_k})$ . The resulting span  
110 can be labeled  $\langle\langle \mathcal{T} | \chi \rangle\rangle$  (see example in Fig. 3). [The double angle brackets reinforce the  
111 idea that the definition of “display” has changed]

112 **Theorem 2** (Terraces—Type II). *If the score function,  $s$ , satisfies the second condition  
113 required for Theorem 1 (linear sum of costs), and the first condition is modified so that  
114  $c(T, g) = c(T||_{X_g}, g)$ , then every tree in the restriction span,  $\langle\langle \mathcal{T} | \chi \rangle\rangle$ , has the score,  $s(T, \mathcal{G})$ .*

115 *Proof.* The proof follows easily by substituting the restriction span and restriction subtree  
116 operations in the proof for Theorem 1  $\square$

117 The example in Fig. 3 shows that there can be more than one tree on this kind of  
118 terrace, as with the first type of terrace. The elements of  $\langle\langle \mathcal{T} | \chi \rangle\rangle$  and  $\langle \mathcal{T} | \chi \rangle$  are not

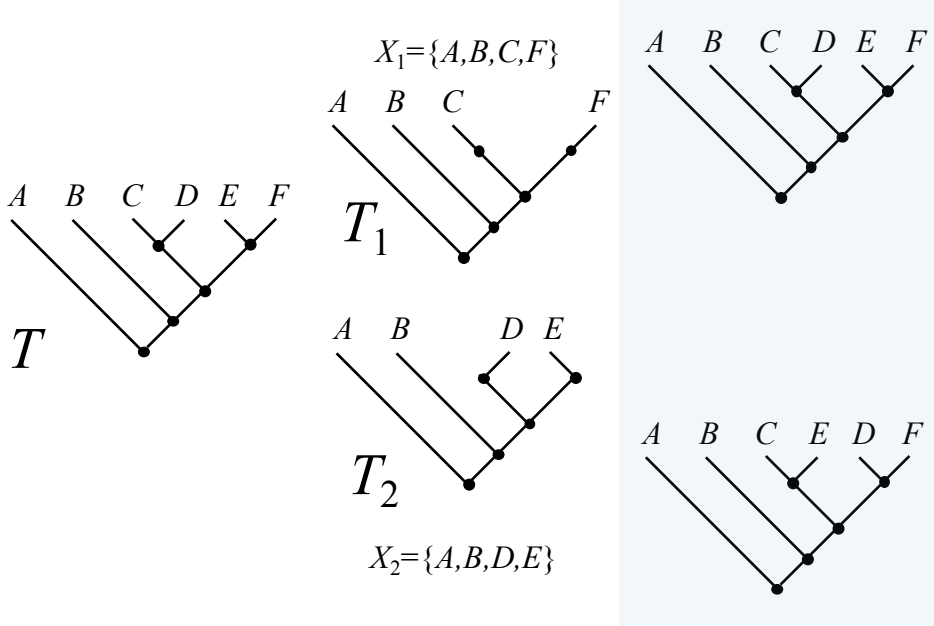


Fig. 3. Restriction span of a set of subtrees. Original rooted parent tree is  $T$  having leaf label set,  $X = \{A, B, C, D, E, F\}$ . Subsets of label sets,  $X_1, X_2 \subseteq X$ , induce “restriction” subtrees (Fig. 1),  $\mathcal{T}||_\chi = (T||_{X_1}, T||_{X_2}) = (T_1, T_2)$ . Each of the trees in the shaded box displays both  $T_1$  and  $T_2$ , and this set of two trees is the *restriction span*,  $\langle\langle \mathcal{T}||_\chi \rangle\rangle$ .

necessarily the same. For example, in Fig. 3 there are 15 trees in  $\langle\langle \mathcal{T}||_\chi \rangle\rangle$  but only two in  $\langle\langle \mathcal{T}||_\chi \rangle\rangle$ . In general, the former set of trees contains the latter, as we now state:

**Theorem 3.** *For any rooted binary parent tree,  $T$ , having leaf label set  $X$ , and given label sets  $\chi = (X_1, \dots, X_k)$ ,  $X_i \subseteq X$ ,*

$$\langle\langle \mathcal{T}||_\chi \rangle\rangle \subseteq \langle\langle \mathcal{T}||_\chi \rangle\rangle. \quad (4)$$

123

*Proof.* Suppose that  $T' \in \langle\langle \mathcal{T}||_\chi \rangle\rangle = \langle\langle T||_{X_1}, \dots, T||_{X_k} \rangle\rangle$ . Then  $T'||_{X_i} = T||_{X_i}$  for all  $i = 1, \dots, k$  and so  $T'|_{X_i} = T|_{X_i}$  for each  $i$  (since restriction display implies ordinary display) and thus  $T' \in \langle T|_{X_1}, \dots, T|_{X_k} \rangle = \langle\langle \mathcal{T}||_\chi \rangle\rangle$ .

127

In parallel with the terminology for terraces, we refer to these two spans as “Type I” and “Type II” respectively. □

130 *Species Tree Inference by Reconciliation*

131 Different regions of the genome can have different phylogenetic histories, and these  
132 “gene trees” can also differ from the species tree in which they are imbedded (Bravo et al.  
133 2019; Liu et al. 2019). The framework of gene tree “reconciliation” provides an analytically  
134 rich and empirically powerful toolkit to understand this mosaic of histories and to infer  
135 species trees from discordant gene trees (Goodman et al. 1979; Page 1994). Here we extend  
136 our previous results on terraces to the reconciliation setting by discussing conditions under  
137 which reconciliation-based score functions lead to terraces when there are missing leaves in  
138 the gene trees.

139 Reconciliation algorithms are based on costs that reflect (at least) four kinds of  
140 explicitly *evolutionary* processes in the phylogenetic history of a gene tree imbedded in a  
141 species tree, “speciation”, “duplication”, “deletion”, and “deep coalescence”. In addition,  
142 costs may reflect some aspect of *sampling* of leaves (Page 1994; Page and Charleston  
143 1997). Additional evolutionary events, such as lateral transfer, have been studied to a  
144 lesser extent (Bansal et al. 2012) but are not considered here. Assume there is a rooted  
145 binary species tree,  $S$ , leaf labeled by  $\mathcal{L}_S$ , and an imbedded rooted binary gene tree,  $g$ ,  
146 labeled by  $\mathcal{L}_g \subseteq \mathcal{L}_S$ . In general, all reconciliation cost functions can be written as  $c(S, g)$ ,  
147 and these are generally combined additively across gene trees, so the score function  $s(T, \mathcal{G})$   
148 discussed above extends easily in principle, even though the underlying sequence data are  
149 no longer relevant.

150 Define a *reconciliation* of  $S$  and  $g$ , loosely, as an annotation of  $g$  that indicates the  
151 locations of speciation events, duplications and losses. [More formal definitions include  
152 defining a *reconciled tree* as an extension of  $g$  made by inserting “lost” subtrees so that the  
153 resulting tree is consistent with speciation and duplication alone (Chauve and El-Mabrouk  
154 2009).]

155 Given a set of gene trees,  $\mathcal{G}$ , the *species tree inference problem* is then to find a

156 species tree,  $\hat{S}$ , that minimizes

$$s(S, \mathcal{G}) = \sum_{g_i \in \mathcal{G}} c(S, g_i) \quad (5)$$

157 over all  $S$ , for various choices of the cost function,  $c(S, g_i)$ .

158 *Incompleteness, missing data, absence, deletion and loss*

159 Let  $\mathcal{L}_{S \setminus g}$  be the set of leaf labels of  $S$  missing from  $g$ . If  $\mathcal{L}_{S \setminus g} \neq \emptyset$ , then  $g$  is  
160 *incomplete*. The concept of “missing data” in the original notion of terraces equates to  
161 incompleteness in one or more gene trees, and this can lead to terraces in the species tree  
162 inference problem.

163 However, distinguishing between evolutionary events and sampling processes can be  
164 confounded in incomplete gene trees. In a gene tree having no leaves from species  $x$ , were  
165 these genes evolutionarily deleted, or was  $x$  never sampled? For  $x \in \mathcal{L}_{S \setminus g}$ , by  
166 “incompleteness due to deletion”, we mean that the absence of  $x$  from  $g$  is considered  
167 positive evidence that no such leaves exist in  $g$  ( $x$  has been well studied and its absence is  
168 meaningful)—absence implies deletion. By “incompleteness due to sampling”, we mean  $x$   
169 has not been studied, and we make no claim a priori about whether further study of  $x$   
170 would reveal it has leaves in  $g$ —absence implies no more than failure to sample or bad lab  
171 technique (Bayzid and Warnow 2018).

172 Page and Charleston (1997) pointed out that the loss cost could influence species  
173 tree inference under reconciliation and thereby raised the issue of how its interpretation  
174 could matter. Bayzid and Warnow (2018) showed, in fact, that the correct loss score of a  
175 gene tree reconciled with a species tree depends directly on this assumption about the  
176 meaning of loss. We therefore qualify the term “loss” by whichever mechanism is assumed  
177 to generate it.

178 *Reconciliation Costs, Incompleteness and Spans*

179 When  $g$  is complete, it is well known that an optimal reconciliation exists that  
 180 minimizes the number of duplications, losses, and duplications plus losses (Chauve and  
 181 El-Mabrouk 2009). The solution can be found using the *MRCA-mapping*,  $\mathcal{M}$ , from node  $u$   
 182 in  $g$  to a node in  $S$ :  $\mathcal{M}_S(u) = \text{MRCA}_S(C_g(u))$ , which identifies the lowest node on the  
 183 species tree that can have the subtree of  $g$  rooted at  $v$  imbedded within it (Fig. 4). Briefly,  
 184 in this optimal reconciliation, a node  $u$  on  $g$  is annotated as a duplication if  $\mathcal{M}_S(u)$  maps  
 185 to the same node of  $S$  that one of the child nodes of  $u$  does. The duplication cost,  $c_{\text{dup}}$ , is  
 186 the number of such duplications. Determining the location of, and the number of losses,  
 187  $c_{\text{loss}}$ , is just slightly more complicated, and depends on lengths of paths mapped onto  $S$   
 188 from  $g$  using  $\mathcal{M}_S(v)$ . The duplication plus loss cost is then  $c_{D+L} = c_{\text{dup}} + c_{\text{loss}}$ . All of these  
 189 computations have been described in detail elsewhere (e.g. Zhang 2011; Bayzid and  
 190 Warnow 2018) and we omit them here.

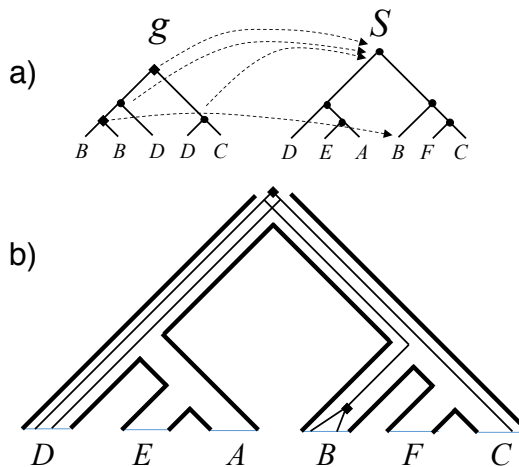


Fig. 4. Reconciliation of a gene tree,  $g$ , and species tree,  $S$ . Note the set of “missing leaves” on  $g$ ,  $\mathcal{L}_{S \setminus g} = \{A, E, F\}$ .  
 a) The MRCA mapping,  $\mathcal{M}$ , is shown for all internal nodes of  $g$ . Nodes annotated as duplications on  $g$  indicated by diamonds; nodes annotated as speciation indicated by dots. b) Imbedding of  $g$  in  $S$ . For clarity, only the duplication nodes on  $g$  are shown as annotated.

191 There are multiple formulations of the deep coalescence cost (Zhang 2011; Steel  
 192 2016),  $c_{DC}$ , which is the number of “extra edges” of the gene tree imbedded within the  
 193 species tree for this reconciliation. Any edge  $e = (u, v) \in E(g)$  is imbedded in  $k_S(e) \geq 0$

<sup>194</sup> edges of  $S$  where  $k_S(e)$  is the number of edges in the path from  $\mathcal{M}_S(u)$  to  $\mathcal{M}_S(v)$ , so the  
<sup>195</sup> number of extra edges is,

$$\sum_{e \in E(g)} k_S(e) - |E(S)| \quad (6)$$

<sup>196</sup> since there is minimally one edge in each edge of  $E(S)$ .

<sup>197</sup> The computation of these reconciliation costs for incomplete gene trees depends in  
<sup>198</sup> part on the interpretation of incompleteness.

<sup>199</sup> *Incompleteness due to sampling.*— The trees  $g$  and  $S|_g$  have the same label sets  
<sup>200</sup> and standard reconciliation algorithms can be used to compute  $c(S|_g, g)$ , but how do we  
<sup>201</sup> compute  $c(S, g)$ ? If the absence of a gene tree leaf for some species taxon is assumed to  
<sup>202</sup> arise because of failure to sample it, we compute the cost,  $c(S, g)$ , by “completing” the  
<sup>203</sup> gene tree so it has the same label set as the species tree (Bayzid and Warnow 2018). A  
<sup>204</sup> *completion*,  $g'$ , is the tree obtained from  $g$  by adding subtree(s) having all the leaves,  
<sup>205</sup>  $x \in \mathcal{L}_{S \setminus g}$ . An *optimal completion*,  $g^*$ , with respect to some cost function,  $c$ , is the  
<sup>206</sup> completion that minimizes  $c$  over all  $g'$ . For example, the optimal completion with respect  
<sup>207</sup> to the duplication cost would be that gene tree,  $g^*$ , that has smallest number of  
<sup>208</sup> duplications among all possible completions. The optimal completion is a guess about  
<sup>209</sup> unsampled leaves that disturbs the cost the least. From here on, when discussing optimal  
<sup>210</sup> completions for incomplete gene trees, we use as shorthand,  $c(S, g)$ , instead of  $c(S, g^*(g))$ .

<sup>211</sup> Bayzid and Warnow (2018) show that there are optimal completions for the  
<sup>212</sup> duplication and loss scores, which have the same duplication and loss scores as that for  
<sup>213</sup>  $c(S|_g, g)$ , so that:

$$c_{dup}(S, g) = c_{dup}(S|_g, g) = c_{dup}(S||_g, g), \quad (7a)$$

$$c_{loss}(S, g) = c_{loss}(S|_g, g), \quad (7b)$$

<sup>214</sup> which implies that the duplication plus loss cost,  $c_{D+L}$  can be obtained simply by adding  
<sup>215</sup> these together. Notice the subtree operation for the loss cost is the homomorphic subtree

216 operation.

217 This can be shown by the following argument. Each unary node,  $u$ , of  $S||_g$   
 218 corresponds to a binary node on  $S$  that has one pendant subtree,  $t$ , the leaves of which are  
 219 all in  $\mathcal{L}_{S \setminus g}$  (i.e., missing). If there are  $l$  edges of  $g$  passing through  $u$ , then we attach  $l$   
 220 replicate instances of  $t$  along their respective edges of  $g$  at new nodes  $v_i, i = 1, \dots, l$ , of  $g$ .  
 221 For each  $v_i$ , the mapping,  $\mathcal{M}(v_i)$  must be to a different node in  $S$  than either the parent of  
 222  $v_i$  maps to, or any of its children map to, because the leaves of  $t$  are in  $\mathcal{L}_{S \setminus g}$ . Thus there  
 223 are no additional duplications inferred by this completion. This argument holds equally for  
 224 both subtree operations, so  $c_{dup}(S|_g, g) = c_{dup}(S||_g, g)$ .

225 This completion also avoids adding  $l$  losses, by “imputing” just the right leaves to  
 226 be present as subtrees of  $g$  (Fig. 5). The loss cost is computed on  $S|_g$  but not  $S||_g$ . The  
 227 intuition for this is that adding these “ghost” subtrees,  $t$ , at edges of  $g$  passing through  $u$   
 228 allows us to pretend, with respect to losses, that node  $u$  was never there.

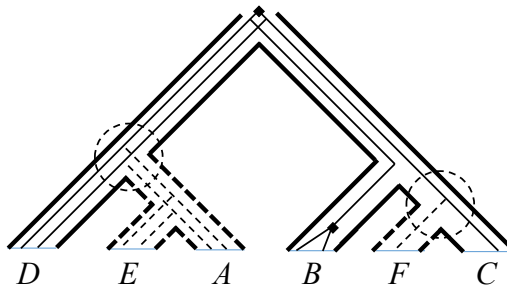


Fig. 5. Optimal completion under the duplication-loss costs. Trees are the same as in Fig. 4. Dashed border for some species tree edges indicates parts of  $S$  that are missing from  $g$  because of absence of leaves  $A, E, F$ . Dashed circles are unary nodes on the restriction subtree,  $S||_g$ . Dashed edges of  $g$  represent the optimal completion of  $g$  that allows leaves of  $g$  to be “present” at leaves of  $S$ , while adding as few duplications and losses as possible to the reconciliation. Here, no duplications or losses are added by this completion. Note that for the unary node at left, two edges of  $g$  traverse it and two subtrees are added, whereas for the unary node at right having one imbedded edge, only one subtree need be added.

229 For the deep coalescence cost when incompleteness is assumed due to sampling we  
 230 can also use the optimal completion approach (Bayzid and Warnow 2012, 2018)(Fig. 6).  
 231 First note that the argument above regarding duplications remains true and no new  
 232 duplications need be added by this completion. Now at each unary node,  $u$ , of  $S||_g$ ,  
 233 however, we attach only one instance of  $t$  to the  $l \geq 1$  edges of  $g$  passing through  $u$ . The

234 remaining  $l - 1$  edges split at  $u$  but immediately are lost (and the interpretation of loss does  
 235 not matter). This guarantees that at most one edge of  $g$  will be present in  $t$  and therefore  
 236 the DC cost will not increase relative to what it was with respect to  $S||g$ , which means

$$c_{DC}(S, g) = c_{DC}(S||_g, g), \quad (8)$$

which, from Eq. 6, means

$$c_{DC}(S, g) = \sum_{e \in E(g)} k_{S||_g}(e) - |E(S||_g)|.$$

237 Note that this is not necessarily an optimal completion for *losses*, as it is fine to add  
 238 losses in order to keep deep coalescences to a minimum.

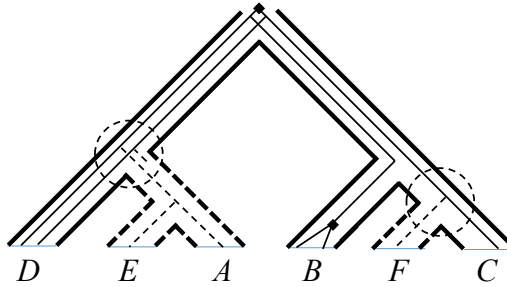


Fig. 6. Optimal completion under the deep coalescence cost. Layout is the same as in Fig. 5. Here the optimal completion must add as few “extra edges” as possible (i.e., over and above one edge of  $g$  per edge of  $S$ ), regardless of how many losses are then required. Note the loss of one edge of  $g$  immediately after its split within the unary node of  $S$  at lower left. Contrast with Fig. 5.

239 *Incompleteness due to deletion.*— Here the absence of a gene tree leaf is assumed  
 240 to be caused by evolutionary deletion of that gene somewhere in the tree. With this  
 241 assumption, we still have

$$c_{dup}^-(S, g) = c_{dup}^-(S|_g, g) = c_{dup}^-(S||_g, g), \quad (9)$$

242 (Chauve et al. 2008; Górecki and Tiuryn 2006; Bayzid and Warnow 2018), where we add  
 243 the superscript  $(-)$  to  $c$  to refer to the deletion interpretation of absence. Duplications are  
 244 unaffected by the choice of subtree operations, because  $\mathcal{M}$  does not map nodes of  $g$  to  
 245 unary nodes of  $S$ , and these nodes are the only difference between  $S|_g$  and  $S||_g$ .

246 But the same is not true for the loss cost (Bayzid and Warnow 2018). The correct

247 count of losses when incompleteness is due to deletion is computed by substituting  $S$  for

248  $S|_g$  in Theorem 3 of Bayzid and Warnow (2018). This computation uses lengths of paths

249 on  $S$  that run from some node  $\mathcal{M}_S(u)$  to  $\mathcal{M}_S(v)$ , where  $u, v$  is a child and parent node on

250  $g$ . Together, all paths in  $S$  of this type comprise the tree,  $S||_g$ , which means

$$c_{loss}^-(S, g) = c_{loss}^-(S||_g, g). \quad (10)$$

251 So, unlike the duplication cost, the loss cost is not necessarily the same under the two  
252 interpretations of incompleteness. In fact, they differ exactly by which kind of subtree  
253 operation is appropriate. Bayzid and Warnow (2018, Thm. 4) give an example in which  
254 these different interpretations of loss lead to different optimal species trees when using the  
255 loss cost.

256 Bayzid and Warnow (2018) also discussed the special case in which missing leaves

257 are distributed on the gene tree in a way that might imply a gene is absent from the root  
258 of the species tree (Fig. 7). This is not a problem when incompleteness is assumed to arise  
259 from sampling, but if it is assumed to arise from deletion, it is necessary to make an

260 assumption about whether genes are present at the root. Let  $u^* = \mathcal{M}_S(r(g))$  be the  
261 location on  $S$  of the root of  $g$ . If  $r(S) > u^*$ , should we assume the gene is present at  $r(S)$ ?

262 In the above treatment, the definition of  $S||_g$  solves the loss problem under the assumption  
263 that a gene is unambiguously present only in the subtree of  $S$  having  $u^*$  as its root. To  
264 make the stronger assumption that it is present at  $r(S)$ , we can define yet another subtree  
265 operator,  $S||_g^r$ , which is the smallest subtree of  $S$  containing  $r(S)$  and the leaf labels of  $g$ .

266 The original restriction operator,  $S||_g$ , can be interpreted in this problematic boundary  
267 case to imply losses are due to deletion in the subtree of  $S$  having  $u^*$  as its root, and losses  
268 are due to sampling elsewhere. We do not pursue this further here, but see Bayzid and  
269 Warnow (2018).

270 The deep coalescence cost when incompleteness is assumed to arise from deletions

271 parallels the case for incompleteness due to sampling. On  $S||_g$ , any unary node,  $u$ , has

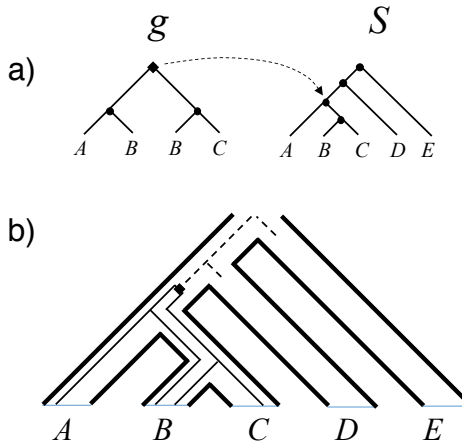


Fig. 7. Special case in which presence of gene at the root of the species tree is ambiguous for incompleteness due to deletion. a) Incomplete gene tree and species tree with MRCA mapping ( $\mathcal{M}$ ) from root of  $g$  shown. b) Imbedding of  $g$  in  $S$  leaving uncertainty toward the root of  $S$ . Dashed lines represent presence of gene if it is forced present at root of  $S$  and location of two losses entailed as a consequence.

272  $l \geq 1$  edges of  $g$  passing through it. To explain the missing leaves present in the pendant  
 273 subtree,  $t$ , of  $u$  that is present on  $S$  but not  $S||g$ , each of these  $l$  lineages must branch at  $u$   
 274 and end in a deletion somewhere in  $t$ . Moreover, at most one edge of  $g$  can persist in  $t$ , else  
 275 there is a deep coalescence and the DC cost is increased. This lineage must end in a  
 276 deletion before reaching a leaf node of  $S$ , and in fact it can be deleted immediately after  
 277 splitting without changing the DC score, because if an edge of  $S$  has no imbedded edges of  
 278  $g$ , its DC score is still zero. In this respect the final form of  $g$  can differ from the optimal  
 279 completion under sampling, but the net result is the same. All missing leaves can be  
 280 accounted for without adding to the DC cost (though perhaps adding to the number of  
 281 losses), and thus the DC cost is the same as for incompleteness due to sampling:

$$c_{DC}^-(S, g) = c_{DC}^-(S||g, g) = c_{DC}(S||g, g) \quad (11)$$

282 *Reconciliation and Terraces*

283 Based on the reconciliation costs for incomplete gene trees in Eqs. 7-11 above and  
 284 Theorem 2, we can summarize which combinations of costs and interpretations of losses  
 285 can lead to terraces (Table 1). First, recall that, from Theorem 3, for a given input, the

286 Type II span of trees is a subset of the Type I span. This implies that if a given  
287 reconciliation setting induces Type I terraces (so that scores are the same for all trees in its  
288 span), then all trees in the corresponding Type II span will also have the same score and  
289 be a Type II terrace. The reverse is not necessarily true.

290 In view of this, all four of the reconciliation costs can lead to Type II terraces and  
291 some, in addition, lead to Type I terraces. The duplication cost can lead to both kinds of  
292 terraces regardless of the interpretation of incompleteness. In contrast, the DC cost can  
293 only lead to Type II terraces (also regardless of the interpretation of incompleteness). For  
294 the loss cost, the nature of the assumption about incompleteness determines which type of  
295 terrace is possible.

296 **DISCUSSION**

297 Terraces in tree space can have several deleterious impacts on phylogenetic  
298 inference (reviewed in Sanderson et al. 2015), and the basic finding that terraces can arise  
299 in tree inference problems under very general conditions (Steel 2016) suggests some care is  
300 warranted. Loosely speaking, these conditions involve missing data and an optimality score  
301 that is decomposable into additive contributions from different subsets of the data.

302 Originally, terraces were shown to arise in multilocus sequence alignments using maximum  
303 parsimony or maximum likelihood optimization scores (Sanderson et al. 2011). In the  
304 latter, certain subsets of models lead to terraces and others do not (Sanderson et al. 2011,  
305 2015). Theory (Sanderson et al. 2010) predicted that terraces in these contexts are most  
306 likely for data sets with many taxa and few loci. A recent meta-analysis (Dobrin et al.  
307 2018) confirms this expectation and indicates the number of trees on terraces can be very  
308 large.

309 It is no surprise that other classes of data sets and optimality criteria used in  
310 phylogenetics that also give rise to terraces. In this paper we explored how terraces can  
311 arise in gene tree reconciliation approaches to species tree inference. Here the gene trees

312 take the place of the multiple sequence alignments of individual loci studied in our earlier  
313 work (Sanderson et al. 2011), and the optimality scores are additive functions of  
314 reconciliation costs that depend on the processes assumed to connect gene trees and  
315 species trees. These vary depending on whether processes of gene duplication, loss or  
316 incomplete lineage sorting are assumed to occur.

317 In considering these divergent biological processes, we found a variant of our  
318 original phylogenetic terrace that is relevant to some but not all of these processes. For  
319 example, under the deep coalescence score, there can be terraces of the second type, but  
320 not of the original type described in Sanderson et al. (2011). The composition of trees on a  
321 terrace—the “span”—is determined by the pattern of missing data in the input. The span  
322 of the trees on a terrace for the deep coalescence score is a subset of the span for the  
323 original type of terrace (which would be a terrace for a different optimality score), and  
324 therefore the size of this kind of terrace is always less than or equal to terraces of the first  
325 type. This implies that the “problem” of terraces should be less for the deep coalescence  
326 score than the duplication score, for example.

327 The phylogenomics literature contains relatively few studies that infer species trees  
328 from gene trees subject to duplication and loss (Sanderson and McMahon 2007; Burleigh  
329 et al. 2011), compared to those that infer species trees in the context of deep coalescence  
330 (e.g. Copetti et al. 2017). For the latter, however, there are a variety of model based and  
331 discrete algorithm approaches to inference (Liu et al. 2019), whereas our results are most  
332 directly relevant to the simple method of minimizing the deep coalescence score (Maddison  
333 1997; Ma et al. 2001; Zhang 2011; Nakhleh 2013). However, we expect that the general  
334 idea of terraces will likely extend to certain model based methods of species tree inference  
335 by analogy with how it extends to likelihood based inference from multi-locus sequence  
336 alignments (Sanderson et al. 2011, 2015). It remains to be seen whether the ultimate  
337 impact of this on species tree inference methods is as dramatic as it is for many large but  
338 sparse multiple sequence alignments (Dobrin et al. 2018).

339 REFERENCES

340 Bansal, M., E. Alm, and M. Kellis. 2012. Efficient algorithms for the reconciliation problem  
341 with gene duplication, horizontal transfer and loss. *Bioinformatics* 28:i283–i291.

342 Bayzid, M. S. and T. Warnow. 2012. Estimating optimal species trees from incomplete  
343 gene trees under deep coalescence. *Journal of Computational Biology* 19:591–605.

344 Bayzid, M. S. and T. Warnow. 2018. Gene tree parsimony for incomplete gene trees:  
345 addressing true biological loss. *Algorithms for Molecular Biology* 13:1–12.

346 Bravo, G. A., A. Antonelli, C. D. Bacon, K. Bartoszek, M. P. K. Blom, S. Huynh,  
347 G. Jones, L. L. Knowles, S. Lamichhaney, T. Marcussen, H. Morlon, L. K. Nakhleh,  
348 B. Oxelman, B. Pfeil, A. Schliep, N. Wahlberg, F. P. Werneck, J. Wiedenhoeft,  
349 S. Willows-Munro, and S. V. Edwards. 2019. Embracing heterogeneity: coalescing the  
350 Tree of Life and the future of phylogenomics. *PeerJ* 7.

351 Burleigh, J. G., M. S. Bansal, O. Eulenstein, S. Hartmann, A. Wehe, and T. J. Vision.  
352 2011. Genome-scale phylogenetics: Inferring the plant tree of life from 18,896 gene trees.  
353 *Systematic Biology* 60:117–125.

354 Chauve, C., J. P. Doyon, and N. El-Mabrouk. 2008. Gene family evolution by duplication,  
355 speciation, and loss. *Journal of Computational Biology* 15:1043–1062.

356 Chauve, C. and N. El-Mabrouk. 2009. New Perspectives on Gene Family Evolution: Losses  
357 in Reconciliation and a Link with Supertrees vol. 5541 of *Lecture Notes in Computer  
358 Science* Pages 46–+.

359 Copetti, D., A. Búrquez, E. Bustamante, J. L. M. Charboneau, K. L. Childs, L. E.  
360 Eguiarte, S. Lee, T. L. Liu, M. M. McMahon, N. K. Whiteman, R. A. Wing, M. F.  
361 Wojciechowski, and M. J. Sanderson. 2017. Extensive gene tree discordance and  
362 hemiplasy shaped the genomes of North American columnar cacti. *Proc. Natl. Acad.  
363 Sci., USA* 114:12003–12008.

REFERENCES

19

364 Dobrin, B. H., D. J. Zwickl, and M. J. Sanderson. 2018. The prevalence of terraced  
365 treescapes in analyses of phylogenetic data sets. *BMC Evolutionary Biology* 18.

366 Felsenstein, J. 2004. Inferring Phylogenies. Sinauer Press, Sunderland, MA.

367 Goodman, M., J. Czelusniak, G. W. Moore, A. E. Romeroherrera, and G. Matsuda. 1979.  
368 Fitting the gene lineage into its species lineage, a parsimony strategy illustrated by  
369 cladograms constructed from globin sequences. *Systematic Zoology* 28:132–163.

370 Górecki, P. and J. Tiuryn. 2006. DLS-trees: A model of evolutionary scenarios. *Theoretical  
371 Computer Science* 359:378–399.

372 Liu, L., C. Anderson, D. Pearl, and S. Edwards. 2019. Modern phylogenomics: Building  
373 phylogenetic trees using the multispecies coalescent model. *Methods in Molecular  
374 Biology* 1910:211–239.

375 Ma, B., M. Li, and L. Zhang. 2001. From gene trees to species trees. *SIAM J. Comput.*  
376 30:729–752.

377 Maddison, W. P. 1997. Gene trees in species trees. *Systematic Biology* 46:523–536.

378 Nakhleh, L. 2013. Computational approaches to species phylogeny inference and gene tree  
379 reconciliation. *Trends in Ecology and Evolution* 28:719–728.

380 Page, R. D. M. 1994. Maps between trees and cladistic analysis of historical associations  
381 among genes, organisms and areas. *Systematic Biology* 43:58–77.

382 Page, R. D. M. and M. A. Charleston. 1997. From gene to organismal phylogeny:  
383 Reconciled trees and the gene tree/species tree problem. *Molecular Phylogenetics and  
384 Evolution* 7:231–240.

385 Sanderson, M., M. M. McMahon, A. Stamatakis, D. J. Zwickl, and M. Steel. 2015. Impacts  
386 of terraces on phylogenetic inference. *Syst. Biol.* 64:709–726.

387 Sanderson, M. J. and M. M. McMahon. 2007. Inferring angiosperm phylogeny from EST  
388 data with widespread gene duplication. *BMC Evolutionary Biology* 7 (Suppl. 1):S3.

389 Sanderson, M. J., M. M. McMahon, and M. Steel. 2010. Phylogenomics with incomplete  
390 taxon coverage: the limits to inference. *BMC Evolutionary Biology* 10.

391 Sanderson, M. J., M. M. McMahon, and M. Steel. 2011. Terraces in phylogenetic tree  
392 space. *Science* 333:448–450.

393 Steel, M. 2016. *Phylogeny: Discrete and Random Processes in Evolution*. SIAM,  
394 Philadelphia.

395 Zhang, L. X. 2011. From gene trees to species trees II: Species tree inference by minimizing  
396 deep coalescence events. *IEEE-ACM Transactions on Computational Biology and*  
397 *Bioinformatics* 8:1685–1691.

Table 1. *Reconciliation Costs and Possible Terrace Types*

Cost/Interpretation of loss	Sufficient Conditions for Terraces of Type
Duplication/Sampling	I,II
Duplication/Deletion	I,II
Loss/Sampling/	I,II
Loss/Deletion	II
D+L/Sampling	I,II
D+L/Deletion	II
DC/Sampling	II
DC/Deletion	II